

Deformed two-dimensional rogue waves in the (2+1)-dimensional Korteweg-de Vries equation

Yulei Cao(曹玉雷), Peng-Yan Hu(胡鹏彦), Yi Cheng(程艺), and Jingsong He(贺劲松)
Citation: Chin. Phys. B, 2021, 30 (**3**): 030503. DOI: 10.1088/1674-1056/abd15e
Journal homepage: http://cpb.iphy.ac.cn; http://iopscience.iop.org/cpb

What follows is a list of articles you may be interested in

Interaction properties of solitons for a couple of nonlinear evolution equations

Syed Tahir Raza Rizvi, Ishrat Bibi, Muhammad Younis, and Ahmet Bekir
Chin. Phys. B, 2021, 30 (**1**): 010502. DOI: 10.1088/1674-1056/abaed3

Localized characteristics of lump and interaction solutions to two extended Jimbo-Miwa equations

Yu-Hang Yin(尹宇航), Si-Jia Chen(陈思佳), and Xing Lü(吕兴)
Chin. Phys. B, 2020, 29 (**12**): 120502. DOI: 10.1088/1674-1056/aba9c4

Stable soliton propagation in a coupled (2+1) dimensional Ginzburg-Landau system

Li-Li Wang(王丽丽), Wen-Jun Liu(刘文军)
Chin. Phys. B, 2020, 29 (**7**): 070502. DOI: 10.1088/1674-1056/ab90ea

Lump, lumpoff and predictable rogue wave solutions to a dimensionally reduced Hirota bilinear equation

Haifeng Wang(王海峰), Yufeng Zhang(张玉峰)
Chin. Phys. B, 2020, 29 (**4**): 040501. DOI: 10.1088/1674-1056/ab75d7

Soliton structures in the (1+1)-dimensional Ginzburg-Landau equation with a parity-time-symmetric potential in ultrafast optics

Wenyi Li(李文义), Guoli Ma(马国利), Weitian Yu(于维天), Yujia Zhang(张玉佳), Mengli Liu(刘孟丽), Chunyu Yang(杨春玉), Wenjun Liu(刘文军)
Chin. Phys. B, 2018, 27 (**3**): 030504. DOI: 10.1088/1674-1056/27/3/030504

Deformed two-dimensional rogue waves in the (2+1)-dimensional Korteweg–de Vries equation*

Yulei Cao(曹玉雷)[1], Peng-Yan Hu(胡鹏彦)[2,†], Yi Cheng(程艺)[3], and Jingsong He(贺劲松)[1]

[1] *Institute for Advanced Study, Shenzhen University, Shenzhen* 518060, *China*
[2] *College of Mathematics and Statistics, Shenzhen University, Shenzhen* 518060, *China*
[3] *School of Mathematical Sciences, University of Science and Technology of China, Hefei* 230026, *China*

(Received 12 October 2020; revised manuscript received 29 November 2020; accepted manuscript online 8 December 2020)

Within the $(2+1)$-dimensional Korteweg–de Vries equation framework, new bilinear Bäcklund transformation and Lax pair are presented based on the binary Bell polynomials and gauge transformation. By introducing an arbitrary function $\phi(y)$, a family of deformed soliton and deformed breather solutions are presented with the improved Hirota's bilinear method. By choosing the appropriate parameters, their interesting dynamic behaviors are shown in three-dimensional plots. Furthermore, novel rational solutions are generated by taking the limit of the obtained solitons. Additionally, two-dimensional (2D) rogue waves (localized in both space and time) on the soliton plane are presented, we refer to them as deformed 2D rogue waves. The obtained deformed 2D rogue waves can be viewed as a 2D analog of the Peregrine soliton on soliton plane, and its evolution process is analyzed in detail. The deformed 2D rogue wave solutions are constructed successfully, which are closely related to the arbitrary function $\phi(y)$. This new idea is also applicable to other nonlinear systems.

Keywords: two-dimensional (2D) Korteweg–de Vries (KdV) equation, Bilinear method, Bäcklund transformation, Lax pair, deformed 2D rogue wave

PACS: 05.45.Yv, 02.30.Jr, 02.30.Ik **DOI:** 10.1088/1674-1056/abd15e

1. Introduction

Rogue waves (RWs) in the ocean, also known as killer waves, monster waves, freak waves, and extreme waves, are special waves with extremely destructive, which should be responsible for some maritime disasters. The main feature of RW is that "appear from nowhere and disappear without a trace".[1] Peregrine was the first one who obtained the RW solution from one-dimensional systems,[2] so such RW solution is also called "Peregrine soliton". These RWs are localized in both space and time in one-dimensional systems,[3–9] and its dynamic behaviors are similar to that of lumps in high-dimensional systems.[10–14] RWs in high-dimensional systems are often called line RWs, which are merely localized in time.[15–18] The study of RW has been widely used in diverse areas of theoretical and applied physics, including plasma physics,[19,20] Bose–Einstein condensates,[21,22] atmosphere physics,[23] optics and photonics,[24–26] and superfluids.[27]

Now, a fundamental problem can be asked: Is it possible that other types of RW solutions exist in nonlinear systems? Seeking new exact solutions for nonlinear systems is an open problem and a challenging work. Furthermore, in integrable systems, the Peregrine soliton only appears in the one-dimensional systems. But, the RWs, which are localized in time and space, have never been found in the high-dimensional system. Therefore, searching for the RW solution that is local in time and space in high-dimensional systems has always been an open problem. Until recently, Guo *et al.*[28] obtained RW solutions, which are localized in both space and time, from a two-dimensional nonlinear Schrödinger model by the even-fold Darboux transformation. Now the long-standing problem of the construction of two-dimensional (2D) rogue wave on zero background has been addressed.[28] This is a pioneering work, which inspires us to explore the structure of 2D RW solutions of other high-dimensional soliton equations. Additionally, the RW solutions of complex nonlinear equations have been widely researched, but the RW solutions of real nonlinear equations are rarely mentioned, which is another motivation.

Inspired by the above considerations, in this paper, we focus on the $(2+1)$-dimensional Korteweg–de Vries (KdV) equation

$$U_t + U_{xxx} - 3(UV)_x = 0, \quad U_x = V_y, \tag{1}$$

which was first derived by Boiti–Leon–Manna–Pempinelli with a weak Lax pair,[29] and can be reduced to the celebrated KdV equation if $x = y$. Equation (1) is an asymmetric part of the Nizhnik–Novikov–Veselov (NNV) equation,[30] thus equation (1) is also called ANNV equation; this equation can also be derived by using the inner parameter-dependent symmetry constraint of the KP equation,[30] and can be considered as a model of an incompressible fluid where U and V are the components of velocity.[31] Equation (1) was also

*Project supported by the National Natural Scinece Foundation of China (Grant Nos. 11671219, 11871446, 12071304, and 12071451).
†Corresponding author. E-mail: pyhu@szu.edu.cn
© 2021 Chinese Physical Society and IOP Publishing Ltd

regarded as a generalization[32] of the results of Hirota and Satsuma[33] in the $(2+1)$ dimensions.

Let $U = W_y$, $V = W_x$, then equation (1) reduces to the following single equation:

$$W_{yt} + W_{xxxy} - 3W_{xx}W_y - 3W_xW_{xy} = 0. \tag{2}$$

Equation (2) known as BLMP equation was widely investigated. The Cauchy problem, associated with initial data decaying sufficiently rapidly at infinity, was solved by means of inverse scattering transformation.[29] The spectral transformation, nonclassical symmetries, and Painlevé property for Eq. (2) have been studied in Refs. [29,34,35]. And a series of Bäcklund transformations,[36–38] Lax pairs,[38] supersymmetric,[39] soliton-like,[40–43] breather,[44,45] and lump-type[46–48] solutions were derived.

In this paper, we are committed to exploring new Bäcklund transformations, Lax pairs, and new RW solutions of 2D KdV equation (1) by the Hirota method. The new RW solution is called deformed 2D RW because its formula involves an arbitrary function $\phi(y)$ which provides a deformed background for the rogue wave. This arbitrary function $\phi(y)$ comes from the crucial bilinear transformation which maps U to a bilinear form. In Section 2, new Bäcklund transformations and Lax pair are derived based on the binary Bell polynomials and linearizing the bilinear equation. In Section 3, we obtain the deformed kink soliton and deformed breather solutions of the 2D KdV equation by means of the Hirota method. In Section 4, a family of new rational solutions and deformed 2D RW solutions of Eq. (1) are presented by introducing an arbitrary function $\phi(y)$. The main results of the paper are summarized and discussed in Section 5.

2. Bilinear Bäcklund transformation and associated Lax pair

In this section, we mainly focus on the new Bäcklund transformation and Lax pair of 2D KdV equation (1). Bäcklund transformation and lax pair are recognized as the main characteristics of integrability, which can be used to obtain exact solutions of nonlinear systems. We first introduce the following variables transformation:

$$U = -q_{xy}, \quad V = -q_{xx}, \tag{3}$$

then 2D KdV equation (1) becomes

$$E(q) = q_{yt} + q_{xxxy} + 3q_{xx}q_{xy} = 0, \tag{4}$$

two different solutions $q = 2\ln G$ and $\widetilde{q} = 2\ln F$ of Eq. (1) are introduced, the corresponding two-field condition is as follows:[49–53]

$$\begin{aligned} &E(\widetilde{q}) - E(q) \\ &= (\widetilde{q}-q)_{yt} + (\widetilde{q}-q)_{xxxy} + 3(\widetilde{q}_{xx}\widetilde{q}_{xy} - q_{xx}q_{xy}) = 0. \end{aligned} \tag{5}$$

We introduce two new variables

$$v = \frac{\widetilde{q}-q}{2} = \ln\frac{F}{G}, \quad w = \frac{\widetilde{q}+q}{2} = \ln FG. \tag{6}$$

Based on the binary Bell polynomials, equation (5) can be rewritten into $\mathcal{Y}$-polynomials from Bell polynomial theory as follows (see Refs. [51–53] for details):

$$\begin{aligned} &E(\widetilde{q}) - E(q) \\ &= 2[v_{yt} + v_{xxxy} + 3w_{xx}v_{xy} + 3w_{xy}v_{xx}] \\ &= 2[\partial_y(\mathcal{Y}_{xxx} + \mathcal{Y}_t) + 3w_{xy}v_{xx} - 3w_{xxy}v_x - 3v_x^2v_{xy}]. \end{aligned} \tag{7}$$

We have the following constraints:

$$w_{xy} + v_xv_y - \lambda v_x = 0, \tag{8}$$

where λ is the constant parameter. Then, the following coupled system of $\mathcal{Y}$-polynomials of Eq. (1) is deduced:

$$\begin{aligned} &\mathcal{Y}_{xy} - \lambda\mathcal{Y}_x = 0, \\ &\mathcal{Y}_{xxx} + \mathcal{Y}_t = 0. \end{aligned} \tag{9}$$

According to the relationship between $\mathcal{Y}$-polynomials[51–53] and bilinear operators D[54]

$$\begin{aligned} &\mathcal{Y}_{n_1x_1,\cdots,n_lx_l}(v = \ln\frac{F}{G}, w = \ln FG) \\ &= (FG)^{-1}D_{x_1}^{n_1}\cdots D_{x_l}^{n_l}F\cdot G, \end{aligned} \tag{10}$$

the following bilinear Bäcklund transformation is derived for the 2D KdV equation (1):

$$\begin{aligned} &(D_xD_y - \lambda D_x)F\cdot G = 0, \\ &(D_x^3 + D_t)F\cdot G = 0. \end{aligned} \tag{11}$$

Then logarithmic linearization of $\mathcal{Y}$-polynomials under the Hopf–Cole transformation $v = \ln\psi$, and Bell polynomial formula

$$\begin{aligned} &(FG)^{-1}D_{x_1}^{n_1}\cdots D_{x_l}^{n_l}F\cdot G\Big|_{G=\mathrm{e}^{\frac{q}{2}},\frac{F}{G}=\psi} \\ &= \sum_{r_1+\cdots+r_l=\text{even}}\sum_{r_1=0}^{n_1}\cdots\sum_{r_l=0}^{n_l}\prod_{i=1}^{l}\binom{n_i}{r_i}P_{r_1x_1\cdots r_lx_l}(q) \\ &\times\mathcal{Y}_{(n_1-r_1)x_1,\ldots,(n_l-r_l)x_l}(v), \end{aligned} \tag{12}$$

the $\mathcal{Y}$-polynomials can be written as

$$\mathcal{Y}_{n_1x_1,\ldots,n_lx_l}(v) = \frac{\psi_{n_1x_1,\ldots,n_lx_l}}{\psi}, \tag{13}$$

thus system (9) is then linearized into a Lax pair

$$\begin{aligned} &\psi_{xy} + q_{xy}\psi - \lambda\psi_x = 0, \\ &\psi_{xxx} + 3q_{xx}\psi_x + \psi_t = 0, \end{aligned} \tag{14}$$

which is equivalent to the Lax pair of Eq. (1)[36]

$$\psi_{xy} - U\psi - \lambda\psi_x = 0,$$

$$\psi_{xxx} - 3V\psi_x + \psi_t = 0. \tag{15}$$

In order to get a new Bäcklund transformation, we introduce the following gauge transformation to the bilinear Bäcklund transformation (11):

$$F \to \mathrm{e}^{\xi} F, \quad G \to \mathrm{e}^{\eta} G, \tag{16}$$

where $\xi = m_1 x + n_1 y + l_1 t$ and $\eta = m_2 x + n_2 y + l_2 t$. System (11) is transformed into

$$\begin{aligned} &[(D_x + m_1 - m_2)(D_y + n_1 - n_2) - \lambda(D_x + m_1 - m_2)]F \cdot G = 0, \\ &\left[(D_x + m_1 - m_2)^3 + (D_t + l_1 - l_2)\right] F \cdot G = 0, \end{aligned} \tag{17}$$

under the following constraints:

$$m_1 - m_2 = \lambda, \quad n_1 - n_2 = \lambda, \quad l_2 - l_1 = \lambda^3. \tag{18}$$

Then, a new Bäcklund transformation of Eq. (1) is derived as follows:

$$\begin{aligned} &(D_x D_y + \lambda D_y)F \cdot G = 0, \\ &(D_x^3 + 3\lambda D_x^2 + 3\lambda^2 D_x + D_t)F \cdot G = 0. \end{aligned} \tag{19}$$

Similarly, the Lax pair of system (1) is as follows:

$$\begin{aligned} &\psi_{xy} + \lambda\psi_y + q_{xy}\psi = 0, \\ &\psi_{xxx} + 2\lambda\psi_{xx} + 3(\lambda^2 + q_{xx})\psi_x + 3\lambda q_{xx}\psi + \psi_t = 0, \end{aligned} \tag{20}$$

or equivalently

$$\begin{aligned} (L_1 - U)\psi &= \psi_{xy} + \lambda\psi_y - U\psi = 0, \\ (\partial_t + L_2)\psi &= \psi_{xxx} + 2\lambda\psi_{xx} + 3(\lambda^2 - V)\psi_x \\ &\quad - 3\lambda V\psi + \psi_t = 0. \end{aligned} \tag{21}$$

It is easy to check that the integrability condition $[L_1 - U, \partial_t + L_2]\psi = 0$ is satisfied.

Additionally, another form of Bäcklund transformation and lax pair of 2D KdV equation (1) are also derived, when taking

$$U = -2\partial_{xy} \ln f(x,y,t) + \phi(y), \quad V = -2\partial_{xx} \ln f(x,y,t), \tag{22}$$

2D KdV equation (1) is then translated into the following bilinear form:

$$[D_x^3 D_y + D_y D_t - 3\phi(y)D_x^2] f(x,y,t) \cdot f(x,y,t) = 0, \tag{23}$$

where $\phi(y)$ is an arbitrary function of y, f is a real function, and D is the Hirota's bilinear differential operator,[54] based on the binary Bell polynomials,[49–51] equation (1) admits the following Bäcklund transformation:

$$\begin{aligned} &[D_x D_y - \phi(y)]F \cdot G = 0, \\ &\left[D_x^3 + D_t + k\right] F \cdot G = 0. \end{aligned} \tag{24}$$

If using gauge transformation (16) to the above bilinear Bäcklund transformation (24), a new Bäcklund transformation of Eq. (1) is derived

$$\begin{aligned} &\left[D_x D_y + \lambda(D_x + D_y) + \lambda^2 - \phi(y)\right] F \cdot G = 0, \\ &\left[D_x^3 + 3\lambda D_x^2 + 3\lambda^2 D_x + D_t + k\right] F \cdot G = 0. \end{aligned} \tag{25}$$

Then, we derive the corresponding linear system under the Hopf–Cole transformation (13)

$$\begin{aligned} &\psi_{xy} + \lambda(\psi_x + \psi_y) + (\lambda^2 + q_{xy} - \phi(y))\psi = 0, \\ &\psi_{xxx} + 3\lambda\psi_{xx} + 3(\lambda^2 + q_{xx})\psi_x + \psi_t + (3\lambda q_{xx} + k)\psi = 0, \end{aligned} \tag{26}$$

which is equivalent to the Lax system of 2D KdV equation (1)

$$\begin{aligned} &\psi_{xy} + \lambda(\psi_x + \psi_y) + (\lambda^2 - U)\psi = 0, \\ &\psi_{xxx} + 3\lambda\psi_{xx} + 3(\lambda^2 - V)\psi_x + \psi_t + (k - 3\lambda V)\psi = 0. \end{aligned} \tag{27}$$

3. Deformed multi-kink soliton and deformed breather solutions of the 2D KdV equation

Based on the above new bilinear equation (23), some exact solutions of 2D KdV equation (1), including deformed multi-solitons and deformed breathers, are generated. First, the deformed one-soliton solutions take the forms

$$\begin{aligned} U_{[1]} &= -2\partial_{xy} \ln(1 + \mathrm{e}^{\eta_1}) + \phi(y), \\ V_{[1]} &= -2\partial_{xx} \ln(1 + \mathrm{e}^{\eta_1}), \end{aligned} \tag{28}$$

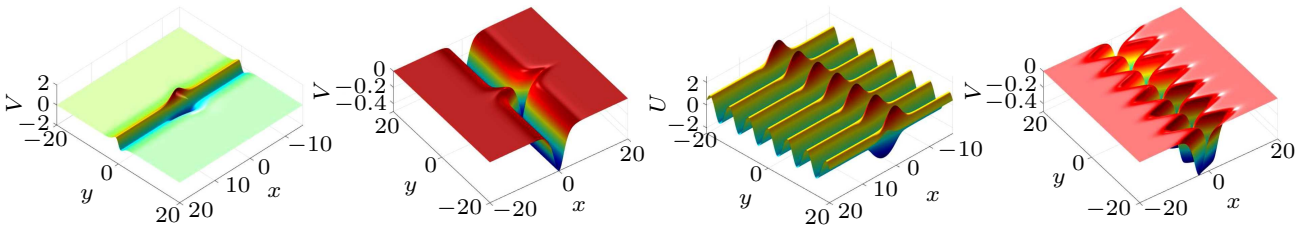
where $\eta_1 = p_1 x + \Phi(y) q_1 y + \Omega_1 t + \eta_1^0$, $\eta_1^0 = 0$, and $\phi(y) = \mathrm{d}\Phi(y)/\mathrm{d}y$. Substituting Eq. (28) into Eq. (1), the following dispersion relation of the 2D KdV equation is obtained:

$$\Omega_1 = -\frac{p_1^2(p_1 q_1 - 3)}{q_1}.$$

The exact expressions of $U_{[1]}$ and $V_{[1]}$ are as follows:

$$\begin{aligned} U_{[1]} &= \phi(y)\frac{1 + \cosh\left(p_1 x + q_1\Phi(y) + (\frac{3p_1^2}{q_1} - p_1^3)t\right) - p_1 q_1}{1 + \cosh\left(p_1 x + q_1\Phi(y) + (\frac{3p_1^2}{q_1} - p_1^3)t\right)}, \\ V_{[1]} &= -\frac{p_1^2}{1 + \cosh\left(p_1 x + q_1\Phi(y) + (\frac{3p_1^2}{q_1} - p_1^3)t\right)}. \end{aligned} \tag{29}$$

As can be seen from the above expression, the extremum lines $p_1 x + q_1\Phi(y) + (3p_1^2/q_1 - p_1^3)t$ and velocity $(3p_1 - q_1 p_1^2)/q_1$ of $U_{[1]}$ and $V_{[1]}$ are the same, and the corresponding amplitudes of $U_{[1]}$ and $V_{[1]}$ in (x,y)-plane are $\phi(y)(1 - (p_1 q_1/2))$ and $p_1^2/2$, respectively. Thus, $U_{[1]}$ is a deformed bright soliton when $\phi(y)(2 - p_1 q_1) > 0$ and a deformed dark soliton when $\phi(y)(2 - p_1 q_1) < 0$. However, $V_{[1]}$ is always a deformed dark soliton see Fig. 1.



(a) $\Phi(y)=\mathrm{sech}(y)$ (b) $\Phi(y)=\mathrm{sech}(y)$ (c) $\Phi(y)=\sin(y)$ (d) $\Phi(y)=\sin(y)$

Fig. 1. Deformed one-soliton $U_{[1]}$ and $V_{[1]}$ of Eq. (1) in the (x,y)-plane with parameters $p_1=1$, $q_1=-4$ and displayed at $t=0$.

In order to obtain the deformed two-solitons of 2D KdV equation (1), we take

$$U_{[2]}=-2\partial_{xy}\ln(1+\mathrm{e}^{\eta_1}+\mathrm{e}^{\eta_2}+\mathrm{e}^{\eta_1+\eta_2+A_{12}})+\phi(y),\quad V_{[2]}=-2\partial_{xx}\ln(1+\mathrm{e}^{\eta_1}+\mathrm{e}^{\eta_2}+\mathrm{e}^{\eta_1+\eta_2+A_{12}}),\tag{30}$$

where $\eta_1=p_1x+\Phi(y)q_1y+\Omega_1t+\eta_1^0$ and $\eta_2=p_2x+\Phi(y)q_2y+\Omega_2t+\eta_2^0$. Substituting Eq. (30) into Eq. (1), the following relations are obtained:

$$\Omega_1=-\frac{p_1^2(p_1q_1-3)}{q_1},\quad \Omega_2=-\frac{p_2^2(p_2q_2-3)}{q_2},\quad \exp(A_{12})=\frac{(p_1q_2-p_2q_1)^2+p_1p_2q_1q_2(p_1-p_2)(q_1-q_2)}{(p_1q_2-p_2q_1)^2+p_1p_2q_1q_2(p_1+p_2)(q_1+q_2)}.\tag{31}$$

Further, by taking $p_1=3$, $q_1=3$, $p_2=\frac{5}{2}$, $q_2=3$, $\eta_1^0=-\eta_2^0=\frac{\pi}{2}$, the analytical expressions $U_{[2]}$ and $V_{[2]}$ of the deformed two-soliton solutions are as follows:

$$U_{[2]}=\frac{\left\{\cosh(2\kappa_{11})-\sinh(2\kappa_{11})+982081\left(\sum\limits_{j=2}^{4}[\cosh(2\kappa_{1j})+\sinh(2\kappa_{1j})]\right)+\left(\sum\limits_{m=1}^{5}\Gamma_m[\cosh(\kappa_m)-(-1)^m\sinh(\kappa_m)]\right)\right\}}{\frac{1}{\phi(y)}\left(\cosh(\kappa_{11})-\sinh(\kappa_{11})+991\sum\limits_{j=2}^{4}[\cosh(\kappa_{1j})+\sinh(\kappa_{1j})]\right)^2},$$

$$V_{[2]}=\frac{\left\{[\cosh(3\Phi(y))+\sinh(3\Phi(y))]\left(\sum\limits_{m=1}^{5}\gamma_m[\cosh(\kappa_m-3(-1)^{m+1}\Phi(y))]-\sum\limits_{m=1}^{5}(-1)^m[\sinh(\kappa_m-3(-1)^{m+1}\Phi(y))]\right)\right\}}{-1982\left(\frac{1}{991}[\cosh(\kappa_{11})-\sinh(\kappa_{11})]+\sum\limits_{j=2}^{4}[\cosh(\kappa_{1j})+\sinh(\kappa_{1j})]\right)^2},\tag{32}$$

where

$$\begin{aligned}
&\kappa_{11}=-\frac{11}{2}x-6\Phi(y)+\frac{75}{8}t-\frac{\pi}{2},\\
&\kappa_{12}=\frac{5}{2}x+3\Phi(y)+\frac{69}{8}t,\quad \kappa_{13}=18t+\frac{\pi}{2},\\
&\kappa_{14}=3x+3\Phi(y),\quad \kappa_1=\kappa_{12}+\kappa_{14},\\
&\kappa_2=\kappa_{11}-\kappa_{12},\quad \kappa_3=\kappa_{12}+\kappa_{13},\\
&\kappa_4=\kappa_{11}-\kappa_{14},\quad \kappa_5=\kappa_{13}+\kappa_{14},\\
&\Gamma_1=1900738,\quad \Gamma_2=-15856,\quad \Gamma_3=-12767053,\\
&\Gamma_4=-12883,\quad \Gamma_5=15713296,\\
&\gamma_1=1112,\quad \gamma_2=36,\quad \gamma_3=24775,\\
&\gamma_4=25,\quad \gamma_5=35676.
\end{aligned}\tag{33}$$

The dynamic behaviors of the deformed two-soliton solutions are more complex and interesting by choosing the appropriate parameter $\phi(y)$ see Fig. 2. Furthermore, as can be seen in the two-dimensional plots of Fig. 2, the interaction of the deformed two-soliton solutions is an elastic collision.

Similarly, N-soliton solutions $U_{[N]}$ and $V_{[N]}$ are given in Eq. (22) of the 2D KdV equation (1), in which f can be written as follows:

$$f=f_{[N]}=\sum_{\mu=0,1}\exp\Big(\sum_{j<k}^{(N)}\mu_j\mu_kA_{jk}+\sum_{j=1}^{N}\mu_j\eta_j\Big),\tag{34}$$

with

$$\begin{aligned}
&\eta_j=p_jx+\Phi(y)q_jy+\Omega_jt+\eta_j^0,\quad \Omega_j=-\frac{p_j^2(p_jq_j-3)}{q_j},\\
&\exp(A_{jk})=\frac{(p_jq_k-p_kq_j)^2+p_jp_kq_jq_k(p_j-p_k)(q_j-q_k)}{(p_jq_k-p_kq_j)^2+p_jp_kq_jq_k(p_j+p_k)(q_j+q_k)},
\end{aligned}\tag{35}$$

where p_j,q_j are arbitrary real parameters, η_j^0 is a complex constant, $\phi(y)$ is an arbitrary function of y, and the subscript j denotes an integer. For higher-order soliton solutions, more deformed solitons will be generated from Eq. (34) with appropriate parameter $\phi(y)$, and its dynamic behavior will be more complex, we will not discuss it here.

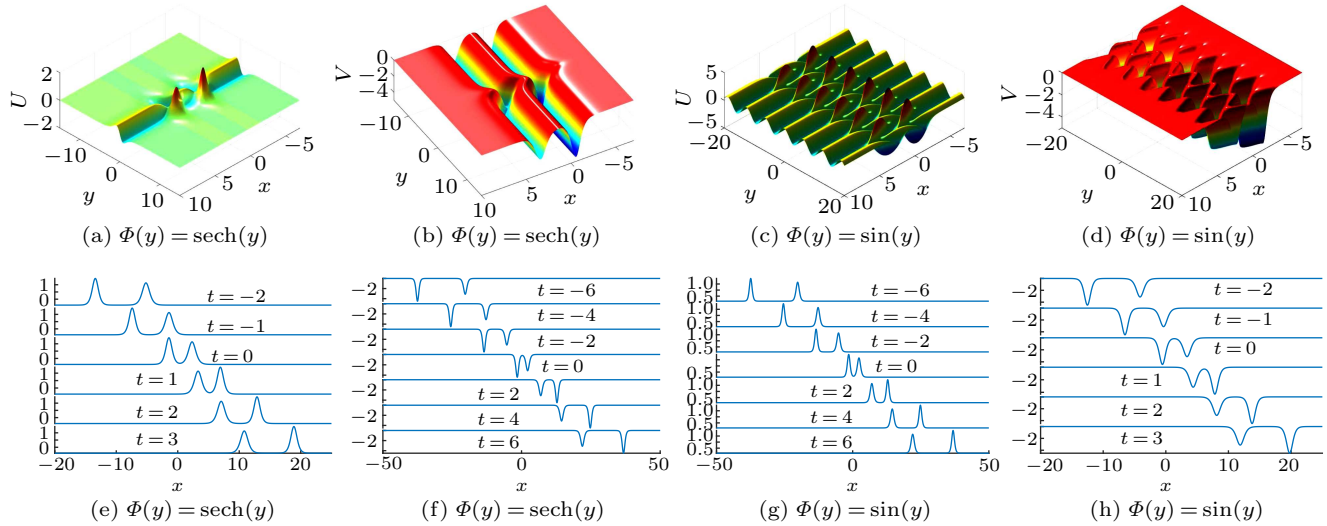


Fig. 2. Deformed two-soliton solutions $U_{[2]}$ and $V_{[2]}$ of Eq. (1) in the (x,y)-plane displayed at $t=0$. Panels (a)–(d) are the two-dimensional plots of (e)–(h), respectively .

4. Deformed 2D RW of the 2D KdV equation

In order to obtain the deformed 2D RW solutions of the 2D KdV equation (1), taking

$$q_1=\lambda_1 p_1,\quad q_2=\lambda_2 p_2,\quad \eta_1^0=\eta_2^0=\mathrm{i}\pi, \tag{36}$$

in Eq. (30) and a suitable limit as $p_1,\ p_2\to 0$, then we further take $\lambda_1=a+b\mathrm{i},\lambda_2=a-b\mathrm{i}$ in Eq. (36). The solutions $U^{[1]}$ and $V^{[1]}$ are given as follows:

$$\begin{aligned}U^{[1]}(x,y,t)&=\phi(y)+4b^2\phi(y)\frac{ab^2(a^2+b^2)A_{21}^2-\frac{b^4}{a}A_{22}^2-A_{23}}{(A_{11}^2+A_{12}^2+A_{13})^2},\\ V^{[1]}(x,y,t)&=4b^2\frac{b^2(a^2-b^2)(a^2+b^2)^2B_{11}^2-\frac{b^4}{a^2-b^2}B_{12}^2-B_{13}}{(A_{11}^2+A_{12}^2+A_{13})^2},\end{aligned} \tag{37}$$

with

$$\begin{aligned}A_{11}&=\frac{3b(a^2-b^2)}{a^2+b^2}t+abx+b(a^2+b^2)\Phi(y),\\ A_{12}&=b^2x+\frac{6ab^2}{a^2+b^2}t,\quad A_{13}=a(a^2+b^2)^2,\\ A_{21}&=\frac{a^2+b^2}{a}x+(a^2+b^2)\Phi(y)+3t,\\ A_{22}&=6at+(a^2+b^2)x, A_{23}=a^2(a^2+b^2)^3,\\ B_{11}&=\frac{a}{a^2-b^2}x+\Phi(y)+\frac{3}{a^2-b^2}t,\\ B_{12}&=6at+(a^2+b^2)x,\quad B_{13}=a(a^2+b^2)^3.\end{aligned} \tag{38}$$

As can be seen from the above expression, to ensure that the above solutions $U^{[1]}$ and $V^{[1]}$ are smooth, parameter $a>0$ must be held.

4.1. Fundamental rational solutions

The fundamental rational solutions $U^{[1]}$ and $V^{[1]}$ of 2D KdV equation (1) are derived if $\phi(y)$ is a polynomial function. Without loss of generality, take $\phi(y)=2y$. The trajectories of $U^{[1]}$ and $V^{[1]}$ are as follows:

$$\begin{aligned}l_1&=ax+(a^2+b^2)y^2+\frac{3(a^2-b^2)}{a^2+b^2}t,\\ l_2&=x+\frac{6a}{a^2+b^2}t.\end{aligned} \tag{39}$$

$\lim\limits_{(x,y)\to\infty}U^{[1]}=2y$ and $\lim\limits_{(x,y)\to\infty}V^{[1]}=0$, which show that the background planes of $U^{[1]}$ and $V^{[1]}$ are $2y$ and 0, respectively. Further, by taking $a=2$ and $b=2$, the exact expression of fundamental rational solutions $U^{[1]}$ and $V^{[1]}$ can be obtained. In order to describe the evolution process of fundamental rational solutions $U^{[1]}$ more clearly, we remove the background plane $2y$ when plotting. As shown in Fig. 3(a), the rational solution $U^{[1]}$ removing the background plane $2y$ appears from a constant plane when $t\ll 0$. With time evolution an arc line $x=-4y^2$ appears on the constant background around $t=0$ [see Fig. (a)], and finally the arc line fissions into a bright lump and a dark lump [see Fig. 3(c)]. The trajectories of the fission are $x+4y^2=0$ and $2x+3t=0$ [see Figs. 3(d)and 3(e)].

However, the dynamic behavior of the rational solution $V^{[1]}$ is different from that of $U^{[1]}$. For given $\phi(y)=2y$, the solution $V^{[1]}$ has the following nine critical points in (x,y)-plane:

$$\begin{aligned}&\Lambda_1=(x_1,y_1)=\left(\frac{3at}{a^2+b^2},y=0\right);\\ &\Lambda_{2,3}=(x_{2,3},y_{2,3})\\ &\quad=\left(\frac{-3abt\pm\sqrt{3a(a^2+b^2)^3+27b^4t^2}}{b(a^2+b^2)},y=0\right);\\ &\Lambda_{4,5}=(x_{4,5},y_{4,5})=\left(-\frac{6at}{a^2+b^2},y=\pm\sqrt{\frac{3t}{a^2+b^2}}\right);\\ &\Lambda_{6,7,8,9}=(x_{6,7,8,9},y_{6,7,8,9})\\ &\quad=\left(\frac{-6abt\pm\sqrt{3a(a^2+b^2)^3}}{b(a^2+b^2)},y=\pm\sqrt{\frac{3t}{a^2+b^2}}\right),\end{aligned} \tag{40}$$

letting

$$\Delta(x,y)=\frac{\partial^2 V^{[1]}}{\partial x^2};$$
$$H(x,y)=\frac{\partial^2 V^{[1]}}{\partial x^2}\frac{\partial^2 V^{[1]}}{\partial y^2}-\left(\frac{\partial^2 V^{[1]}}{\partial x\partial y}\right)^2 \tag{41}$$

yields

$$\Delta(x,y)\Big|_{\Lambda_1}=\frac{24b^4(a^2+b^2)^4}{[a(a^2+b^2)^3+9b^4t^2]^2};$$
$$H(x,y)\Big|_{\Lambda_1}=-\frac{1152b^{10}(a^2+b^2)^7t}{[a(a^2+b^2)^3+9b^4t^2]^4},$$
$$\Delta(x,y)\Big|_{\Lambda_{2,3}}=-\frac{3b^4(a^2+b^2)^4}{4[a(a^2+b^2)^3+9b^4t^2]^2};$$
$$H(x,y)\Big|_{\Lambda_{2,3}}=-\frac{9b^{10}(a^2+b^2)^7t}{2[a(a^2+b^2)^3+9b^4t^2]^4},$$
$$\Delta(x,y)\Big|_{\Lambda_{4,5}}=\frac{24b^4}{a^2(a^2+b^2)^2};$$
$$H(x,y)\Big|_{\Lambda_{4,5}}=\frac{2304b^10t}{a^4(a^2+b^2)^5},$$
$$\Delta(x,y)\Big|_{\Lambda_{6,7,8,9}}=-\frac{3b^4}{4a^2(a^2+b^2)^2};$$
$$H(x,y)\Big|_{\Lambda_{6,7,8,9}}=\frac{9b^{10}t}{a^4(a^2+b^2)^5}. \tag{42}$$

Based on the above analysis, the evolution of rational solution $V^{[1]}$ of 2D KdV equation (1) can be divided into the following three stages.

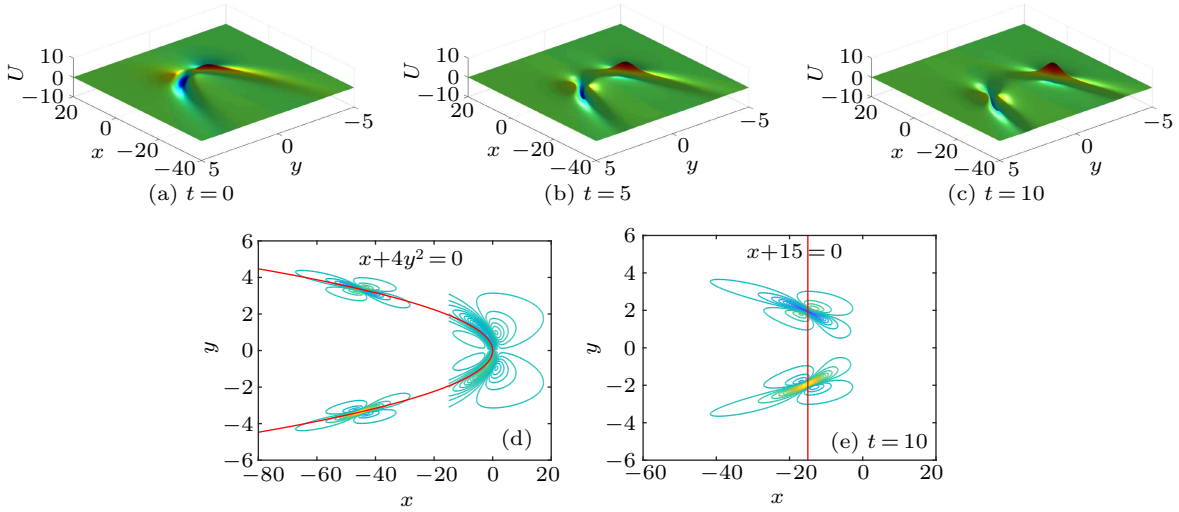


Fig. 3. The temporal evolution of fundamental rational solution $U^{[1]}$ removing the background plane $\phi(y)$ of Eq. (1) in the (x,y)-plane with parameters $\phi(y)=2y, a=2$, and $b=2$. Panels (d) and (e) are two-dimensional plots of $U^{[1]}$.

(i) When $t<0$, $\lim\limits_{(x,y)\to\infty} V^{[1]}=0$, which shows that rational solution $V^{[1]}$ appears from a constant background. Now the maximum value $V^{[1]}_{\max}(x,y)$ and minimum value $V^{[1]}_{\min}(x,y)$ of $V^{[1]}$ are obtained at $\Lambda_{2,3}$ and Λ_1

$$V^{[1]}_{\max}(x,y)=V^{[1]}(x,y)\Big|_{\Lambda_{2,3}}=\frac{b^2(a^2+b^2)^2}{2a(a^2+b^2)^3+18b^4t^2},$$
$$V^{[1]}_{\min}(x,y)=V^{[1]}(x,y)\Big|_{\Lambda_1}=-\frac{4b^2(a^2+b^2)^2}{a(a^2+b^2)^3+9b^4t^2}. \tag{43}$$

Obviously, the global extreme values of rational solution $V^{[1]}$ change with time, and

$$\lim_{t\to-\infty} V^{[1]}_{\max}(x,y)=\lim_{t\to-\infty} V^{[1]}_{\min}(x,y).$$

(ii) When $t=0$, rational solution $V^{[1]}$ has three extreme points

$$A_1(x,y)=(0,0),\quad A_2(x,y)=\left(\frac{\sqrt{3a^2+3ab^2}}{b},0\right),$$
$$A_3(x,y)=\left(-\frac{\sqrt{3a^2+3ab^2}}{b},0\right).$$

The maximum and minimum values are as follows:

$$V^{[1]}_{\max}(x,y)=V^{[1]}(x,y)\Big|_{A_2}=V^{[1]}(x,y)\Big|_{A_3}=\frac{b^2}{2a(a^2+b^2)},$$
$$V^{[1]}_{\min}(x,y)=V^{[1]}(x,y)\Big|_{A_1}=-\frac{4b^2}{a(a^2+b^2)}. \tag{44}$$

From the above analysis, we can seen that its dynamic behavior is similar to the RW in one-dimensional systems. The amplitude of the RW in one-dimensional systems is three times that of the background plane. However, the amplitude of RW of 2D KdV equation (1) is controlled by parameters a and b.

(iii) When $t>0$, rational solution $V^{[1]}$ has six extreme points $\Lambda_{4,5}$ and $\Lambda_{6,7,8,9}$. And it has four maximums and two minimums

$$V^{[1]}_{\max}(x,y)=V^{[1]}(x,y)\Big|_{\Lambda_{6,7,8,9}}=\frac{b^2}{2a(a^2+b^2)},$$

$$V^{[1]}_{\min}(x,y) = V^{[1]}(x,y)\Big|_{\Lambda_{4,5}} = -\frac{4b^2}{a(a^2+b^2)}. \quad (45)$$

Obviously, the extreme values of $V^{[1]}$ at $t=0$ are equal to the extreme values at $t>0$.

Through the above analysis, $|V^{[1]}_{\max}(x,y)| < |V^{[1]}_{\min}(x,y)|$ is always satisfied, which indicates that $V^{[1]}$ is dark. When $t<0$, we know that the rational solution $V^{[1]}$ appears from a constant plane, and the amplitude above the background plane is 8 times of that below the background plane. $V^{[1]}$ reaches the maximum amplitude $\frac{9b^2}{2a(a^2+b^2)}$ at $t=0$. With the time evolution, the dark lump fissions into two identical dark lumps along the curve $ax+(a^2+b^2)y^2+\frac{3(a^2-b^2)}{a^2+b^2}t$. Interestingly, after the dark lump fission into two identical lumps, its amplitude does not change, which means the energy does not change when $t>0$ [see Fig. 4].

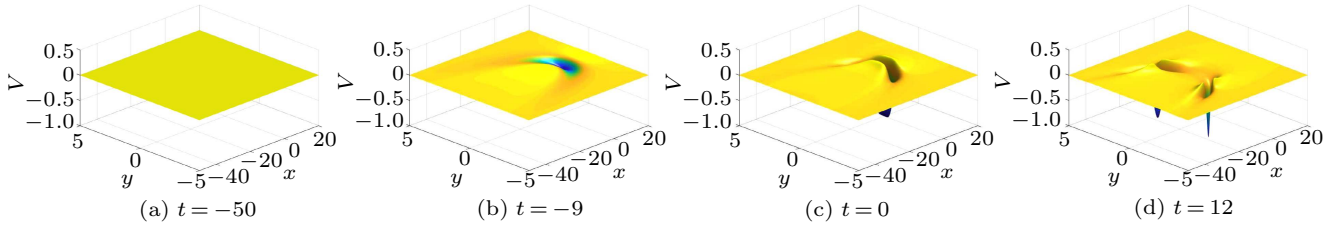


Fig. 4. The temporal evolution of fundamental rational solution $V^{[1]}$ of Eq. (1) in the (x,y)-plane with parameters $\phi(y)=2y, a=2$, and $b=2$.

4.2. Fundamental deformed 2D RW solutions

The fundamental deformed 2D RW $U^{[1]}$ and $V^{[1]}$ of 2D KdV equation (1) are obtained when $\phi(y)=\mathrm{sech}(y)$. $\lim\limits_{(x,y)\to\infty} U^{[1]}=\phi(y)$, which indicated that the background plane of deformed 2D RW $U^{[1]}$ is $\phi(y)$. The trajectories of $U^{[1]}$ are

$$l_1' = ax+(a^2-b^2)\,\mathrm{sech}(y)+3t, \quad l_2' = x+2a\,\mathrm{sech}(y). \quad (46)$$

As can be seen in Fig. 5, in order to better observe the evolution of the deformed 2D RW $U^{[1]}$, we remove the background plane of $U^{[1]}$. Four panels describe the appearance and annihilation of 2D RW in (x,y)-plane along the curve $x+2\,\mathrm{sech}(y)$. This is the first time to obtain such deformed 2D RW in high-dimensional systems. The dynamic behavior of fundamental deformed 2D RW $V^{[1]}$ is more complicated and interesting.

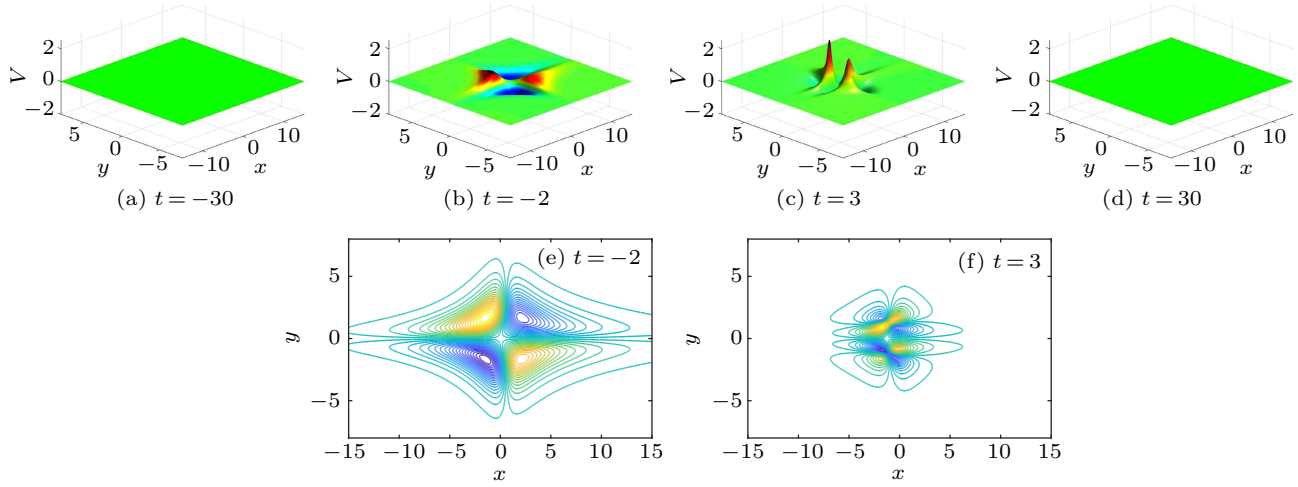


Fig. 5. The temporal evolution of fundamental deformed 2D RW solution $U^{[1]}$ removing the background plane $\phi(y)$ of Eq. (1) in the (x,y)-plane with parameters $\Phi(y)=\mathrm{sech}(y)$, $a=1$, and $b=4$.

Through simple calculation and analysis, the evolution of deformed 2D RW $V^{[1]}$ can be divided into the following four stages

(i) When $t<0$, a line RW appears from the constant background plane, with the time evolution, the amplitude of the line RW gradually increases.

(ii) When $t=0$, the amplitude of the line RW reaches its maximum value. The maximum amplitude $V^{[1]}_{\mathrm{Amp}}$ is

$$V^{[1]}_{\mathrm{Amp}} = V^{[1]}_{\mathrm{Max}} - V^{[1]}_{\mathrm{Min}} = \frac{b^2}{2a(a^2+b^2)} - \frac{-4b^2}{a(a^2+b^2)} = \frac{9b^2}{2a(a^2+b^2)}. \quad (47)$$

(iii) When $0<t\le\frac{a^2+b^2}{3}$, the line RW disappears gradually. Simultaneously, a Peregrine-type soliton is generated, but the amplitude of the RW $V^{[1]}$ is fixed in this process of evolution

(iv) When $t>\frac{a^2+b^2}{3}$, two identical maximum values $V^{[1]}_{\mathrm{Max}}$ and one minimum value $V^{[1]}_{\mathrm{Min}}$ of the Peregrine-type soliton are as follows:

$$V_{\rm Max}^{[1]}=\frac{b^2(a^2+b^2)^2}{2b^4(3t-a^2-b^2)^2+2a(a^2+b^2)^3},\quad V_{\rm Min}^{[1]}=-\frac{4b^2(a^2+b^2)^2}{b^4(3t-a^2-b^2)^2+a(a^2+b^2)^3}. \tag{48}$$

It can be seen from the above expression that the amplitude of the Peregrine-type soliton decays rapidly in a very short time. When $t\gg\frac{a^2+b^2}{3}$, RW $V^{[1]}$ uniformly approaches a constant background see Fig. 6.

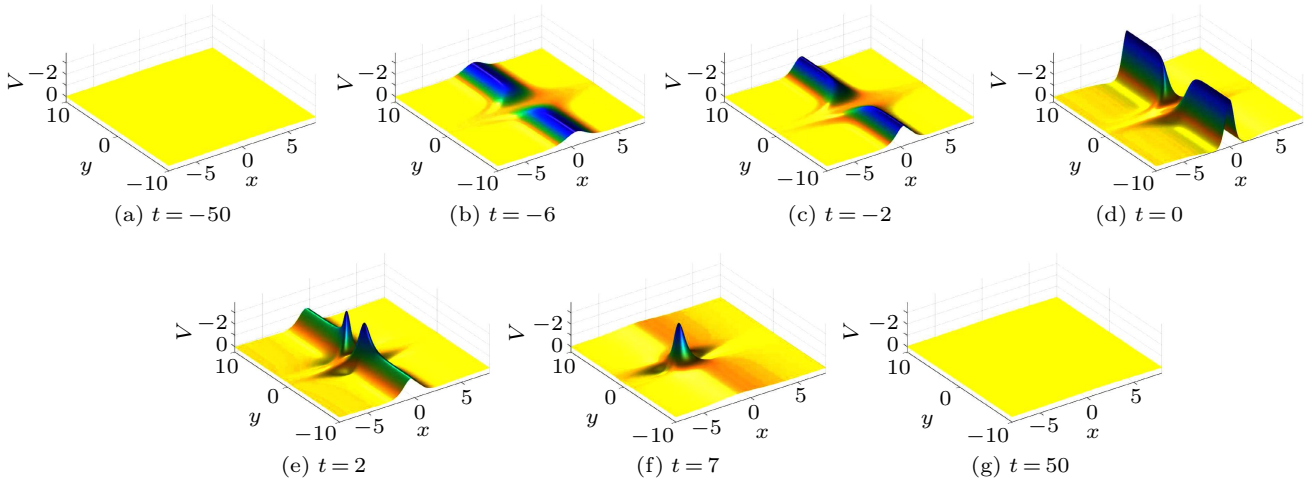


Fig. 6. The temporal evolution of fundamental deformed 2D RW solution $V^{[1]}$ of Eq. (1) in the (x,y)-plane with parameters $\Phi(y)=\mathrm{sech}(y)$, $a=1$, and $b=4$.

4.3. High-order deformed 2D RW solutions

Take

$$N=4,\quad q_j=\lambda_j p_j,\quad \eta_j^0=\mathrm{i}\pi,\quad (j=1,2,3,4), \tag{49}$$

in Eq. (34). Further taking

$$\lambda_1=\lambda_2^*=1+3\mathrm{i},\quad \lambda_3=\lambda_4^*=\frac{1}{2}-4\mathrm{i},$$
$$\Phi(y)=\mathrm{sech}(y), \tag{50}$$

the second-order deformed 2D RW solutions $U^{[2]}=-2\ln f_{xy}^{[2]}+\phi(y)$ and $V^{[2]}=-2\ln f_{xx}^{[2]}$ are generated, in which $f^{[2]}$ can be written as

$$\begin{aligned}
&f^{[2]}(x,y,t)\\
&=x^4+\left[6\Phi(y)+\frac{27}{10}t\right]x^3\\
&\quad+\left[21\Phi(y)^2+\frac{21}{5}\Phi(y)t+\frac{189}{40}t^2+\frac{149877}{1156}\right]x^2\\
&\quad+\left[36\Phi(y)^3+\frac{27}{10}t\Phi(y)^2+\frac{81}{20}t^2\Phi(y)\right.\\
&\quad\left.+\frac{81}{20}t^3+\frac{2924139}{11560}t\right]x\\
&\quad+\frac{81}{40}t^4-\frac{81}{20}\Phi(y)t^3+\left[\frac{801}{40}\Phi(y)^2+\frac{688257}{46240}\right]t^2\\
&\quad+\left[-\frac{144}{5}\Phi(y)^3+\frac{1008648}{1445}\Phi(y)\right]t\\
&\quad+40\Phi(y)^4-\frac{122850}{289}\Phi(y)^2+\frac{1158885}{89}.
\end{aligned} \tag{51}$$

As can be seen in Fig. 7, by removing the background plane $\phi(y)$, the second-order deformed 2D RW solution $U^{[2]}$ describes that four Peregrine-type solitons appear and annihilate from the constant background plane. However, the dynamic behaviors of the second-order RW solution $V^{[2]}$ are similar to that of the fundamental RW solution $V^{[1]}$. The RW solution $V^{[2]}$ uniformly approaches to a constant background plane when $t\to\pm\infty$. Two line RWs appear from the constant plane under the time evolution, and their amplitudes increase rapidly. Then the amplitudes of the two line RW attenuate rapidly, at the same time, two Peregrine-type solitons are produced. Finally, these two Peregrine-type solitons disappear in a very short time without a trace (see Fig. 8).

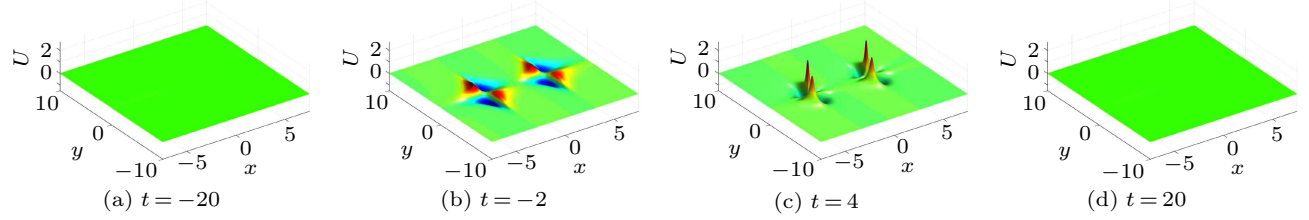


Fig. 7. The temporal evolution of second-order deformed 2D RW solution $U^{[2]}$ removing the background plane $\phi(y)$ of Eq. (1) in the (x,y)-plane.

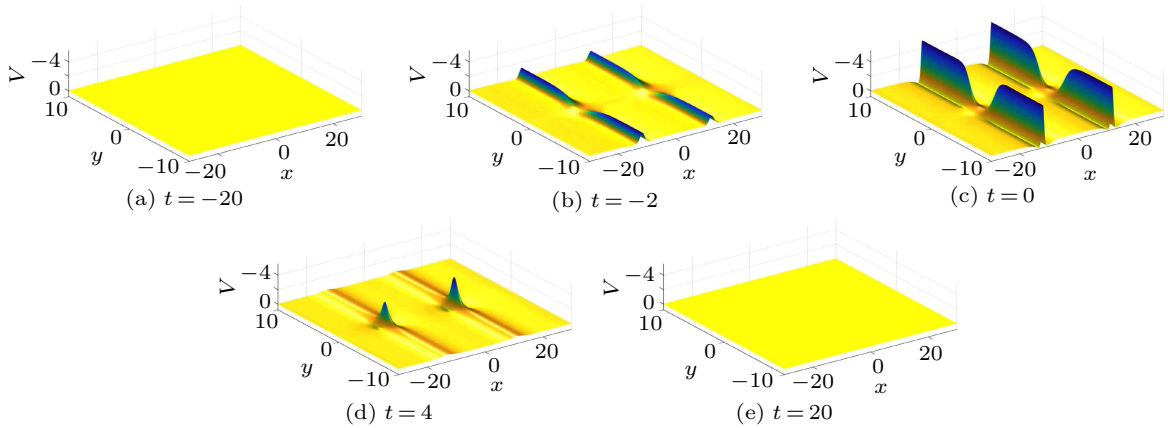


Fig. 8. The temporal evolution of second-order deformed 2D RW solution $V^{[2]}$ of Eq. (1) in the (x,y)-plane.

For larger N, higher-order solutions are generated by taking the parameters

$$N=2n,\quad q_j=\lambda_j p_j,\quad \eta_j^0=\mathrm{i}\pi\quad (1\le j\le N),\tag{52}$$

in Eq. (34) and a suitable long wave limit as $p_j\to 0$, the function f defined in Eq. (34) becomes a polynomial-type function containing an arbitrary function $\phi(y)$. Therefore, the general n-th rational-type functions $U^{[n]}=-2\ln f_{xy}+\phi(y)$ and $V^{[n]}=-2\ln f_{xx}$ of 2D KdV equation (1) can be derived,[55] in which f can be written as follows:

$$\begin{aligned} f=f^{[n]}=&\prod_{k=1}^{N}\theta_k+\frac{1}{2}\sum_{k,j}^{(N)}\alpha_{kj}\prod_{l\neq k,j}^{N}\theta_l+\cdots\\ &+\frac{1}{M!2^M}\sum_{i,j,\ldots,m,n}^{(N)}\overbrace{\alpha_{kj}\alpha_{kl}\cdots\alpha_{mn}}^{M}\prod_{p\neq k,j,\ldots,m,n}^{N}\theta_p+\cdots, \end{aligned}\tag{53}$$

with

$$\theta_j=\frac{\lambda_j^2\phi(y)+\lambda_j x+3t}{\lambda_j},\quad \alpha_{jk}=-\frac{2\lambda_j\lambda_k(\lambda_j+\lambda_k)}{(\lambda_j-\lambda_k)^2},\tag{54}$$

where k and j are two positive integers. We must emphasize that λ_j is a complex constant and $\lambda_j^*=\lambda_{n+j}=a_n+\mathrm{i}b_n$. When $a_n>0$, the above general n-th rational-type functions $U^{[n]}$ and $V^{[n]}$ are smooth.

Remark 1 The above solutions $U^{[n]}$ and $V^{[n]}$ are rational solutions, if $\phi(y)$ is a nonzero polynomial function. For example, when $\phi(y)=2y$, the rational solution $U^{[n]}$ describes the fission of n-bright lumps and n-dark lumps from the background plane $2y$. The rational solution $V^{[n]}$ describes the fission of $2n$-dark lumps from a constant background plane.

Remark 2 The above solutions $U^{[n]}$ and $V^{[n]}$ are deformed 2D RW solutions if $\Phi(y)=\mathrm{sech}(y)$. The solution $U^{[n]}$ describes $2n$ Peregrine-type solitons that appear and annihilate from a kink-soliton plan. The solution $V^{[n]}$ shows that n-line RWs appear and decay rapidly from a constant background plane, and fission into n Peregrine-type solitons, and finally disappear in the constant background plane without a trace.

5. Summary

In this paper, new bilinear Bäcklund transformation and Lax pair of the 2D KdV equation (1) are derived, which are different from the Bäcklund transform and Lax pair in Refs. [36,37]. Teh N-soliton solutions are presented by means of the improved Hirota's bilinear method. Deformed soliton and deformed breather solutions of elastic collision are generated by selecting the appropriate free parameter $\phi(y)$, see Figs. 1 and 2. When $\Phi(y)$ is a non-constant polynomial function, a family of new rational solutions of the 2D KdV equation are generated using the long wave limit. When $\Phi(y)$ ia a non-zero constant, the rational solutions $U^{[n]}$ and $V^{[n]}$ reduce to the rational solution of 2D KdV equation in Ref. [47]. When $\Phi(y)=\mathrm{sech}(y)$, the deformed 2D RW solution U describes a family of Peregrine-type solitons that appear and annihilate from a kink-soliton plan. In order to better observe the evolution of the deformed 2D RW solutions, we remove the background plane of U when plotting, see Figs. 5 and 7. The deformed 2D RW solution V shows that a series of line RWs appear and decay rapidly from a constant background plane, and fission into Peregrine-type solitons, and finally annihilate in the constant background plane without a trace, see Figs. 6 and 8. This paper successfully constructed the deformed 2D RW solutions, which are closely related to the introduced arbitrary function $\Phi(y)$. These novel phenomena have never been reported before in nonlinear systems. Our presented work not only provides a new reference method for seeking new exact solutions of nonlinear partial differential equations, but also may be helpful to promote a deeper understanding of nonlinear phenomena.

References

[1] Akhmediev N, Ankiewicz A and Taki M 2009 *Phys. Lett. A* **373** 675
[2] Peregrine D H 1983 *J. Aust. Math. Soc. B* **25** 16
[3] Guo L J, Wang L H, Cheng Y and He J S 2017 *Commun. Nonlinear Sci. Numer. Simulat.* **52** 11
[4] Zhang Y S, Guo L J, Chabchoub A and He J S 2017 *Rom. J. Phys.* **62** 102

[5] Zhang G Q and Yan Z Y 2018 *Commun. Nonlinear Sci. Numer. Simulat.* **62** 117
[6] He J S, Xu S W and Porsezian K 2012 *Phys. Rev. E* **86** 066603
[7] Li R M, Geng X G and Xue B 2020 *J. Nonlinear Math. Phys.* **27** 279
[8] Yang J and Zhu Z N 2018 *Chaos* **28** 093103
[9] Ling L M, Feng B F and Zhu Z N 2016 *Physica D* **327** 13
[10] Cao Y L, He J S, Cheng Y and Mihalache D 2020 *Nonlinear Dyn.* **99** 3013
[11] Gai L T, Ma W X and Li M C 2020 *Phys. Lett. A* **384** 126178
[12] Rao J G, Zhang Y S, Fokas A S and He J S 2018 *Nonlinerity* **31** 4090
[13] Liu W H, Zhang Y F and Shi D D 2019 *Phys. Lett. A* **383** 97
[14] Rao J G, Wang L H, Liu W and He J S 2017 *Theor. Math. Phys.* **193** 1783
[15] Cao Y L, Malomed B A and He J S 2018 *Chaos Soliton. Fract.* **114** 99
[16] Ohta Y and Yang J K 2013 *J. Phys. A: Math. Theor.* **46** 105202
[17] Rao J G, Mihalache D, Cheng Y and He J S 2019 *Phys. Lett. A* **383** 1138
[18] Zhang Y S, Rao J G, Porsezian K and He J S 2019 *Nonlinear Dyn.* **95** 1133
[19] Elawady E and Moslem W M 2011 *Phys. Plasmas* **18** 082306
[20] Bailung H, Sharma S K and Nakamura Y 2011 *Phys. Rev. Lett.* **107** 255005
[21] Bludov Y V, Konotop V V and Akhmediev N 2009 *Phys. Rev. A* **80** 2962
[22] Bludov Y V, Konotop V V and Akhmediev N 2010 *Eur. Phys. J. Spec. Top.* **185** 169
[23] Stenflo L and Marklund M 2010 *J. Plasma Phys.* **76** 293
[24] Montina A, Bortolozzo U, Residori S and Arecchi F T 2009 *Phys. Rev. Lett.* **103** 173901
[25] Solli D R, Ropers C, Koonath P and Jalali B 2007 *Nature* **450** 1054
[26] Mihalache D 2017 *Rom. Rep. Phys.* **69** 403
[27] Ganshin A N, Efimov V B, Kolmakov G V, Mezhov-Deglin L P and Mcclintock P V E 2008 *Phys. Rev. Lett.* **101** 065303
[28] Guo L J, He J S, Wang L H, Cheng Y, Frantzeskakis D J, Bremer T S and Kevrekidis P G 2020 *Phys. Rev. Research* **2** 033376
[29] Boiti M, Leon J J P, Manna M and Pempinelli F 1986 *Inverse Probl.* **2** 271
[30] Lou S Y and Hu X B 1997 *J. Math. Phys.* **38** 6401
[31] Estevez P G and Leble S 1995 *Inverse Probl.* **11** 925
[32] Leble S B and Ustinov N V 1991 *Inverse Probl.* **10** 617
[33] Hirota R and Satsma J 1994 *J. Phys. Soc. Jpn.* **40** 611
[34] Ablowitz M J and Clarkson P A 1991 *Solitons, Nonlinear Evolution Equations and Inverse Scattering* (Cambridge: Cambridge University Press)
[35] Delisle L and Mosaddeghi M 2013 *J. Phys. A: Math. Theor.* **46** 115203
[36] Lue X, Tian B, Sun K and Wang P 2010 *J. Math. Phys.* **51** 113506
[37] Luo L 2011 *Phys. Lett. A* **375** 1059
[38] Wang C J 2017 *Nonlinear Dyn.* **87** 2635
[39] Clarkson P A and Mansfield E L 1994 *Nonlinearity* **7** 795
[40] Tian B and Gao Y T 1996 *Chaos Soliton Fract.* **7** 1497
[41] Lou S Y 1995 *J. Phys. A: Math. Theor.* **28** 7227
[42] Hu H C, Tang X Y, Lou S Y and Liu Q P 2004 *Chaos Soliton Fract.* **22** 327
[43] Chen Y, Wang Q and Li B 2004 *Commun. Theor. Phys.* **42** 655
[44] Fan E G 2009 *J. Phys. A: Math. Theor.* **42** 095206
[45] Luo L 2010 *Commun. Theor. Phys.* **54** 208
[46] Chen Y R, Song M and Liu Z R 2015 *Nonlinear Dyn.* **82** 333
[47] Liu Y Q and Wen X Y 2019 *Adv. Diff. Equa.* **2019** 332
[48] Wang C J 2016 *Nonlinear Dyn.* **84** 697
[49] Gilson C, Lambert F, Nimmo J and Willox R 1996 *Proc. Roy. Soc. Lond. A* **452** 223
[50] Bell E T 1935 *Ann. Math.* **35** 258
[51] Fan E G 2011 *Phys. Lett. A* **375** 493
[52] Luo L 2019 *Appl. Math. Lett.* **94** 94
[53] Lambert F and Springael J 2001 *Chaos Soliton Fract.* **12** 2821
[54] Hirota R 2004 *The direct method in soliton theory* (Cambridge: Cambridge University Press)
[55] Ablowitz M J and Satsuma J 1979 *J. Math. Phys.* **20** 1496